Fibers and Polymers 2011, Vol.12, No.5, 572-579 DOI 10.1007/s12221-011-0572-8

Carbon Dioxide and Methane Gas Permeations in Thermally Annealed and Chemically Cross-Linked Commercial Polyimide Hollow Fiber Membrane

Grace M. Nisola, Arnel B. Beltran, Viava Jane L. Africa, Eulsaeng Cho[1], Midoek Han, and Wook-Jin Chung*

Energy and Environment Fusion Technology Center, Department of Environmental Engineering and Biotechnology, Myongji University, Yongin 449-728, Korea

[1]*Division of Water and Environmental Strategy Research Group, Korea Environment Institute, Korea*

(Received November 7, 2010; Revised February 28, 2011; Accepted March 5, 2011)

Abstract: Two types of modifications were performed on a commercial polyimide (PI) hollow fiber membrane for carbon dioxide (CO_2) and methane (CH_4) gas permeations. Thermal annealing was conducted between 50- and 200 °C while chemical cross-linking was performed using 0.1- to 1.0 wt% of N, (1-Naphthyl) ethylene-diamine dihydrochloride (NED). Membrane characterization revealed densification of the thermally annealed PIs. But formation of macrovoids was observed in PIs annealed near its glass transition temperature (207 °C). Fourier transform infrared spectroscopy confirmed the successful cross-linking of NED with PI. Highest CO_2 permeance was obtained from pristine PI (P/L=225 GPU) but it also had the lowest selectivity (α=72). The performances of thermally annealed (P/L=160-219 GPU, α=76-106), NED cross-linked (P/L=68-139 GPU, α=65-95) and thermally induced NED cross-linked (P/L=51-91 GPU, α=98-138) PIs varied according to modification conditions. Among the modified membranes, highest CO_2 permeance was obtained from thermally annealed PI at 100 °C (P/L=211GPU, α=106) while thermally induced NED cross-linked PI (100 °C, 0.5 wt% NED) exhibited the highest selectivity (P/L=91, α=138). Both modified membranes are the best candidates for CO_2/CH_4 separation.

Keywords: Polyimide, Hollow fiber, Gas permeation, Carbon dioxide, Methane

Introduction

Biogas typically contains 65 % methane (CH_4) with the presence of carbon dioxide (CO_2) as the major impurity (<35 %) and trace amounts of nitrogen (N_2), oxygen (O_2), hydrogen (H_2) and moisture [1]. Aside from the corrosive property of CO_2 in the presence of moisture, it also lowers the heating value of biogas [2]. Thus, natural gas purification steps are performed to improve the quality of the fuel [3].

One of the most effective methods for CO_2/CH_4 separation is the utilization of gas permeation membranes. While gas membrane separation technology has been established for over three decades, its main persisting drawback lies on the stability of membrane materials [4]. The swelling-induced plasticization of membranes by CO_2 increases polymeric chain mobility which often compromises the membrane selectivity [1].

It has been estimated previously that CO_2/CH_4 gas separation membranes must have selectivities at least 40 to have a better competition with other existing technologies [1,4]. This can be easily achieved if the membrane material has inherently high CO_2/CH_4 selectivities (α) like polyimides (PI). Polyimides have been slowly replacing cellulose acetate, the most common membrane material used for CO_2/CH_4 separation [3,4]. Additionally, PIs are well-known for their chemical resistance and excellent mechanical stability due to their rigid polymeric structure [1,5,6]. However, like other polymeric materials, α of PI membranes deteriorate in the presence of condensable gases like CO_2 and CH_4 due to induced plasticization [6-8].

Numerous methods like synthesis of novel PI polymers [9], thermal annealing [10-12], blending of PI with other materials [13,14], UV irradiation [15], PI in interpenetrating networks [16,17] and chemical cross-linking [1,3,8,18-22] have been investigated to improve the gas transport properties of PI membranes.

Although these techniques were proven successful, most of them cannot be easily advanced to commercial applications. The fastest route to marketability would be to upgrade the properties of commercially available membranes.

Among the available modification methods, thermal annealing and chemical cross-linking are the easiest techniques than can be performed on commercial PI membranes. Kawakami *et al.* [10] showed significant CO_2/CH_4 permselectivity improvements (from 42 to 117) in PI membranes thermally cured at 250 °C. A more recent study showed that CO_2 plasticization of Matrimid® hollow fibers was successfully suppressed by thermal annealing the PI membrane for 30 min at temperature >250 °C [23]. For chemical modifications of PI, room temperature diol, diamine and dendrimers have been used as cross-linking agents and membranes with superior gas separation performances have been produced [1,3,8,18-21,24,25]. Some studies also reported the successful alleviation of induced plasticization by thermal annealing of chemically cross-linked PI membranes [11,19,20]. From these reports, selection of cross-linking reagents is an

*Corresponding author: wjc0828@gmail.com

important step to consider, as it can significantly affect the gas separation performance of the PI membranes [19].

In this study, the gas transport properties of a commercial hollow fiber (HF) PI membrane were conveniently upgraded through thermal annealing, chemical cross-linking and thermally induced chemical cross-linking modifications. The feasibility of a new diamine compound (1-Naphthyl) ethylene-diamine dihydrochloride (NED) as a cross-linking agent was evaluated. The selected HF PI membrane is typically used as N_2 separation membrane and its applicability for CO_2 and CH_4 systems was determined through permeation experiments. Membrane characterizations were performed to confirm the modifications and pure gas permeation experiments of CO_2 and CH_4 were conducted to compare the performances of the modified PI membranes.

Experimental

Materials and Reagents

A commercial HF PI membrane module was purchased from Ube Industries, Ltd., Japan (NM-B02A). The cross-linking agent NED was purchased from Yakuri Pure Chemicals Co., Ltd., Japan while solvent methanol (99 %) of high purity grade was obtained from Duksan Chemicals in South Korea. All reagents were used without further purification.

For pure gas experiments, at least 99.9 % pure nitrogen (N_2), oxygen (O_2), hydrogen (H_2) and CO_2 gases were purchased from Union Gas, South Korea while pure CH_4 was from Deok-yang Gas, South Korea.

Polyimide Membrane Modifications

The commercial PI module was dismantled and portions were taken for various modifications such as (1) thermal annealing, (2) NED cross-linking and (3) thermally induced NED cross-linking.

Thermal annealing of the PI membranes was conducted according to the modified method of Zhou and Koros [12]. The furnace was heated under vacuum condition until it reached the desired temperature (50, 100, 150 or 200 ^{o}C). The PI membranes, encased in a perforated aluminum box, were then quickly placed into the oven 30 min after steady measurements were achieved. Slight temperature drop was observed right after putting the samples but it took only <5 min for the oven to return to the set values. After two hours of heating, the membranes were removed from the furnace, cooled and stored in a dessicator before use.

For NED cross-linking of PI, MeOH solution containing the desired amount (0.1, 0.25, 0.5 or 1.0 w/v %) of NED was prepared. Ample amount of the solution was poured on a 150 mm Pyrex glass dish. The HF membranes were then completely submerged in the solution (without touching one another) to allow uniform cross-linking at 30 ^{o}C. Right after immersion, micro-bubbles appeared but were easily removed by gently tapping the dish. The dish was sealed with paraffin film to assure constant NED concentration during reaction and to prevent MeOH evaporation. After one hour, the membranes were taken out and washed four times using pure MeOH to remove the un-reacted NED. The samples were then vacuum-dried in an oven for two hours at 50 ^{o}C to remove the residual MeOH. Finally, the membrane samples were cooled and stored in a dessicator before use.

For thermally induced NED cross-linking modification, the same steps of NED cross-linking was performed but the MeOH-washed samples were further annealed at different temperatures (100, 150 or 200 ^{o}C) for two hours in a vacuum oven. After the thermal treatment, the samples were cooled and kept in a dessicator.

Membrane Characterization

Dynamic mechanical analysis (DMA; Seiko Exstar 6000) was performed to obtain the transition glass (T_g value) temperature of the membrane. The experiment was performed at a frequency of 1 Hz, the testing temperature ranged from 50 to 425 ^{o}C at heating rate of 10 ^{o}C/min. Membrane morphologies were examined under Field Emission Scanning Electron Microscope (FE-SEM, JEOL JSM7000F) at 5-15 kV accelerating voltage. The membrane samples were inspected at 30,000-50,000X magnifications. The chemical properties of NED cross-linked PI membranes were observed through Fourier Transform Infrared Spectrometer with Attenuated Total Reflectance (FTIR-ATR) (Varian 2000 Scimitar series).

Densities of thermally annealed PI membranes were estimated through a modified pycnometry method, with distilled water used as the reference liquid. A known amount of sample was placed in a pre-weighed pycnometer, which was then partially filled with distilled water. The samples were then placed in a vacuum chamber where alternating vacuum infiltration and dry N_2 gas purging were performed to assist the removal of microbubbles from the membrane. The pycnometer was then completely filled with water and was allowed to equilibrate for five more days in a dry environment (30 ^{o}C) prior to final weighing. This is to assure full penetration of water into the membrane. Measurements were performed in triplicates.

Lab-scale Membrane Module Fabrication

Lab-scale membrane modules were fabricated using poly-urethane (PU) tube, with 8 mm inside diameter, as the module body. Two PU tubes, 3- and 11 cm long, were joined by a tee connector which served as the outlet port of the permeating gas. Each module contained five fibers which were fixed by epoxy on both ends. Gas feed entered the tube side of the membrane at one end of the module while the other end was connected to a high precision gate valve for stage cut control. The effective length of the module was 14 cm and the equivalent total membrane area was 9 cm^2.

Gas Permeation Experiment

Permeation experiments were carried out at 100 % stage cut using pure gas systems of N_2, O_2, H_2, CO_2, and CH_4. For measurements, the permeate stream was connected to a bubble flow meter and readings were manually performed after the system attained a steady state condition, usually after one hour of stabilization. Four membrane modules were tested for permeation and these are: (1) pristine PI, (2) thermally annealed, (3) NED cross-linked, and (4) thermally induced NED cross-linked membranes. All permeation experiments were performed at 30 °C, with feed pressure (p) of 3 atm and downstream pressure of 1 atm. To evaluate the non-ideal behavior of the permeating gas (A) under these operating conditions, gas fugacities (f) were calculated using equation (1) at the given p. Since pure gas permeations were performed, mole fraction (y_A) were equal to 1. Fugacity coefficients (ϕ_A) were estimated using Virial equations of states [26-28]. Because the operating pressure was low, all gases had ϕ values >0.98 at the feed side and >0.99 at the permeate side. Though permeance errors would be minimal if partial pressures are used, equation (2) was still adapted for higher accuracy of results.

$$f = \phi_A y_A p \tag{1}$$

$$\left(\frac{P}{L}\right)_A = \frac{N_A}{(f_{A,feed} - f_{A,permeate})} \tag{2}$$

$$\alpha_{CO_2/CH_4} = \frac{(P/L)_{CO_2}}{(P/L)_{CH_4}} \tag{3}$$

Permeation results were reported as permeance (P/L) which was estimated according to equation (2), where L is the selective layer thickness. The permeating gas flux (N_A) was normalized by the differences in the calculated f values at the feed and permeate streams [29]. All P/L measurements were reported in GPU which is equivalent to $10^{-6}\cdot cm^3\cdot(STP)/cm^2\cdot s\cdot cm\text{-}Hg$ [12]. Ideal selectivities (α) were also calculated according to equation (3).

Results and Discussion

Membrane Characterization: Effect of NED Cross-linking

The molecular structure of the used commercial PI is shown in Figure 1, where the 'Ar' component is an aromatic divalent radical [30]. The PI material is produced by condensation polymerization of biphenyltetracarboxylic dianhydride and aromatic diamines.

The FTIR spectra of NED cross-linked PIs are shown in Figure 2. N, (1-Naphthyl) ethylene-diamine dihydrochloride powder features primary and secondary N-H stretch at 3389 cm^{-1}. The C-H stretch of the naphthyl group is located at 3000-2750 cm^{-1} while C-C stretch and C-H bend are evident at 1520-1420 cm^{-1} [31,32]. Peak of N-H stretch in NED was not observed in cross-linked PIs as its vibrational frequency

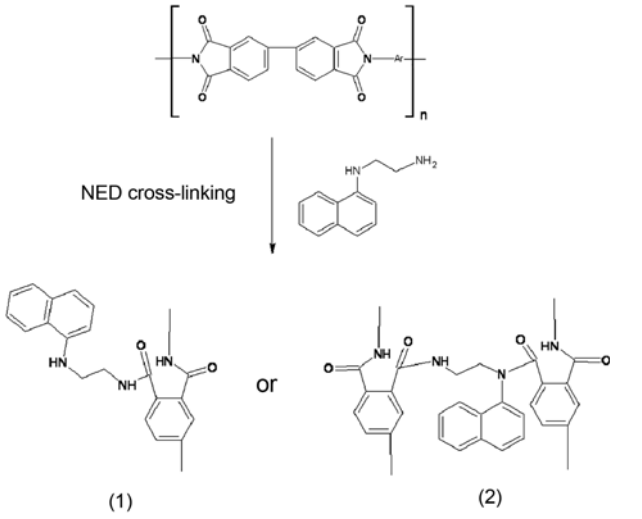

Figure 1. Proposed cross-linking mechanism of NED with PI membrane; (1) NED attached as a pendant molecule and (2) NED cross-linking between PI chains.

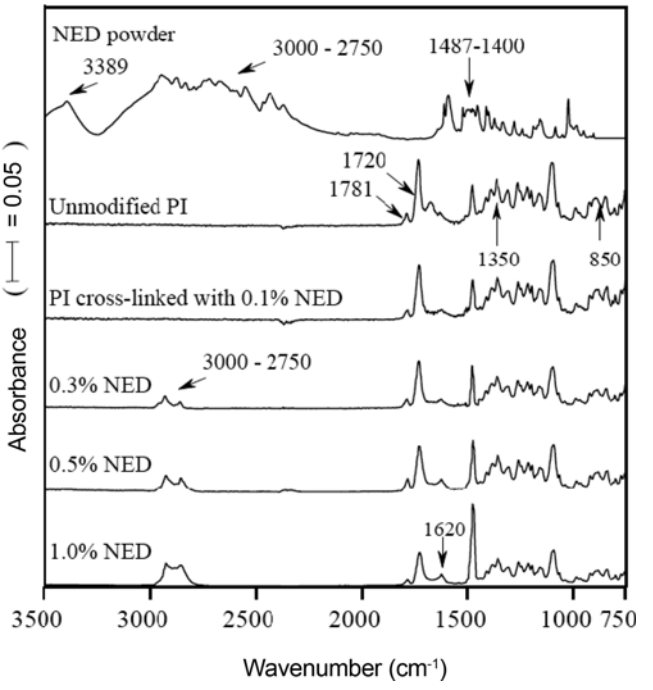

Figure 2. FTIR spectra of chemically cross-linked PI membranes.

is intrinsically weak [33]. With modifications done at low NED concentrations, N-H vibrational stretches in cross-linked PIs were not detected by the FTIR. Characteristic peaks of unmodified PI membranes include asymmetric C=O stretch of imide group at 1781 cm^{-1}, symmetric C=O stretch of the imide group at 1720 cm^{-1}, C-N stretch of the imide group at 1350 cm^{-1} and deformation of imide group at 850 cm^{-1} [20,34]. The intensities of these peaks were lower in NED cross-linked membranes as compared to the

unmodified PI. For example, pristine PI had absorbance value a=1.25 at 1720 cm^{-1} while PI cross-linked with 1 wt% NED only had a=0.71. At 1350 cm^{-1}, unmodified PI had a=0.92 while 1 wt% NED cross-linked PI had a=0.59. As NED concentration increased, peak absorbances associated to the imide group of pristine PI continuously diminished. This suggests that the extent of cross-linking can be increased by increasing NED concentration. This finding was consistent with the observed peak at 3000-2750 cm^{-1} for cross-linked PIs which became more remarkable at increasing NED concentration. This band is associated to the C-H stretch of naphthyl group, a characteristic peak of NED [31,32]. Other indications of successful NED cross-linking are the observed peaks at 1620 cm^{-1} which is related to C=O stretch of amide groups. Unmodified PI had no peak at this frequency while NED cross-linked PIs had subtle peaks with a=0.025. At 1490 cm^{-1}, peaks associated to C-N-H stretch of amide groups were also evident. From a=0.79 of unmodified PI, the peak intensity of cross-linked PI (1 wt% NED) was almost doubled (a=1.58). At increasing NED concentration, more C-N bonds of imide groups were cleaved to form amide during cross-linking [20,25].

Thus, given the results of FTIR spectra, proposed NED cross-linking reaction is shown in Figure 1. There are two ways of which NED could have been incorporated within the PI chains. It is possible that some NEDs were attached to the PI chains as pendant molecules while others acted as cross-linker via amide formation at the cleaved C-N bonds of imide groups [20,25].

In Figure 3, FE-SEM images of pristine and modified membranes are shown. Figures 3(a) and 3(b) show the asymmetric morphology of pristine PI membrane. The dense skin layer can be seen at the outer portion of the HF with an estimated thickness of L=117 nm. On the other hand, the inner part of the tube had a nodular porous structure. The morphology of 0.5 wt% NED cross-linked PI in Figure 3(c) is similar with pristine PI. The slight decrease in skin layer thickness (L=108 nm) can be due to the NED reaction on PI surface and heat treatment at 50 °C. Since no structural irregularity was observed in NED cross-linked PI, FE-SEM results indicate that NED is chemically compatible with the commercial PI and is therefore, a suitable cross-linking agent.

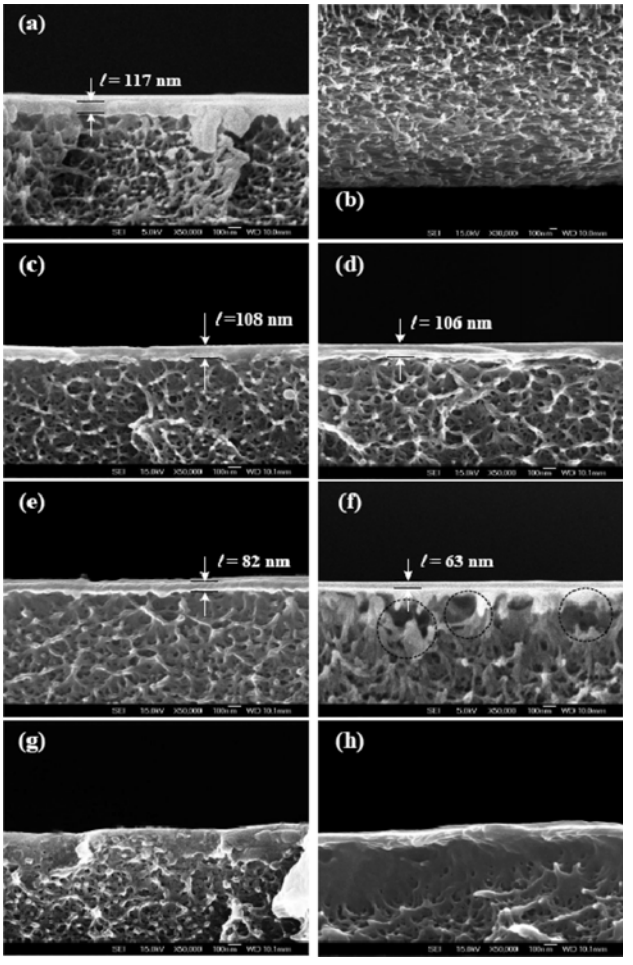

Figure 3. FE-SEM micrographs of bare and modified PI membranes; (a) top, (b) bottom sections of pristine HF PI membrane, (c) 0.5 wt% NED cross-linked PI (d) thermally annealed PI membrane at 100 °C, (e) at 150 °C, (f) at 200 °C, (g) thermally-induced 0.5 wt% NED cross-linked PI at 100 °C, and (h) at 200 °C.

Membrane Characterization: Effect of thermal Annealing

The effect of thermal annealing was investigated through FE-SEM images shown in Figure 3 and density changes in Figure 4. Compared to pristine PI, thermally annealed membranes at 100 °C (Figure 3(d)) and 150 °C (Figure 3(e)) have denser structures. It is also evident that skin layer thickness decreased as annealing temperature is increased. Thermally annealed PI membranes often exhibit densification caused by rearrangement or co-planarization of PI chains

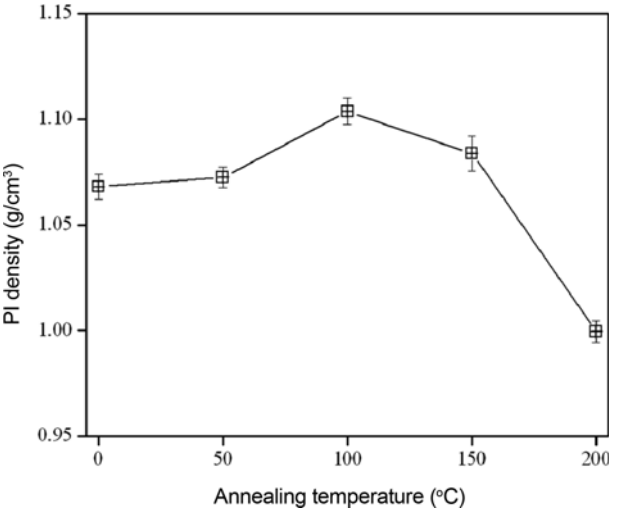

Figure 4. Density of thermally annealed HF PI membranes.

[10,12]. It is known that PI is composed of alternating sequence of electron donor and acceptor monomers [35]. The interaction between PI monomers or chains is referred to as charge transfer complexation (CTC), a typical property exhibited by PIs. The thermally annealed PI membranes showed color change from off-white to amber which is a visual indication of electronic structural rearrangement of the PI polymer chains [20]. During thermal annealing, the inter-planar proximities of PI chains become closer and this facilitated CTC, where p-p electron transfer between the five-member imide- and benzene rings occurred [10-12]. The occurrence of CTC often resulted to a more aggregated structure of PI membrane. The densification of a thermally annealed PI membrane would lower gas permeances, more remarkably on larger gas molecules. This would often result to larger permeance differences which could further improve the selectivity of the membrane [1,3,4]. However at the highest annealing temperature (200 °C), macrovoids subjacent to the skin layer were observed as shown in Figure 3(f).

The density trend in Figure 4 appears to increase with annealing temperature except for PI annealed at 150 °C which was slightly lower than that of PI annealed at 100 °C. But the difference between these samples is within their standard deviations. On the other hand, PI annealed at 200 °C exhibited a remarkably lower density than pristine PI, which is consistent with the FE-SEM results. The lower density of PI annealed at 200 °C is due to the formation of macrovoids within the membrane. To further elucidate the effect of high annealing temperature (200 °C) on the structure of PI, DMA analysis was performed to determine the glass transition temperature (T_g) of the membrane.

Result of DMA in Figure 5 illustrates that the T_g value of the commercial PI was at 207 °C. This is within the range of the reported T_g values for PI polymers which vary between 170 and 500 °C [2,36-37]. As shown in the figure, the onset temperature at which storage modulus declined is at 191 °C. This is the temperature at which of PI started to deform at a given load. Thus, DMA result indicates that annealing temperature of 200 °C (i.e. near PI T_g value) is high enough to cause structural changes in the membrane as evidenced by the presence of macrovoids seen in FE-SEM (Figure 3(f)).

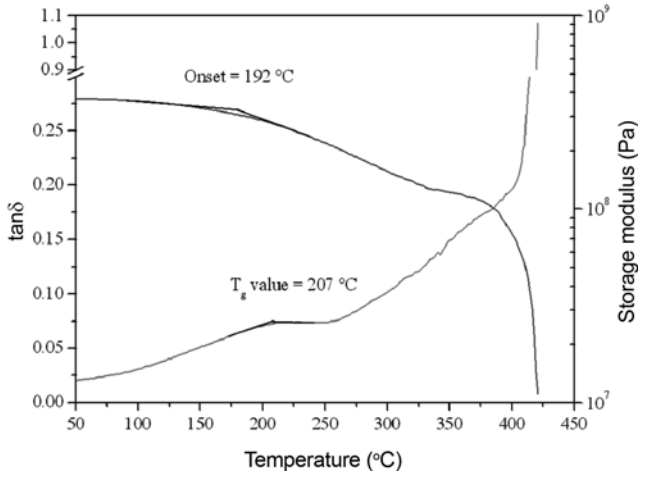

Figure 5. Dynamic mechanical analysis of the commercial PI HF membrane.

Pure Gas Permeations in Pristine HF PI Membrane

The used commercial HF PI membrane was manufactured for O_2/N_2 separation. Permeations of H_2, O_2, N_2, CO_2, and CH_4 on pristine PI were conducted in order to determine the feasibility of the purchased membrane for CO_2/CH_4 apart from O_2/N_2 separation. Additionally, H_2 gas was tested in order to observe the dependence of permeance to the kinetic diameters (k_D) of gas molecules, which is typically exhibited by glassy polymeric membranes like PI [20].

Figure 6 illustrates the permeation results of five gases which can be arranged in the following order: $H_2>CO_2>O_2>N_2>CH_4$. This result consistently demonstrates the indirect relationship between permeance and k_D of gas molecules; smaller gas like H_2 could easily diffuse through the PI membrane as compared bulkier gases like N_2 and CH_4 [20].

The k_D values can also be used to estimate the ideal membrane α. For O_2/N_2 separation, the unmodified HF PI membrane had α value of 6 which was close to the value provided by the manufacturer. Note that the k_D values of O_2 and N_2 vary by 0.2 Å [27]. Thus, considering the larger k_D difference between CO_2 and CH_4 (by 0.5 Å), it is possible to attain (1) higher CO_2 permeance and (2) higher CO_2/CH_4 selectivity. This was confirmed by the obtained CO_2 permeance (P/L=225 GPU) which was >5 times higher than that on O_2 (P/L=42 GPU). Additionally, calculated ideal CO_2/CH_4 selectivity (α=72) shown in Figure 6 was 12 times higher than that of O_2/N_2. These results confirm the

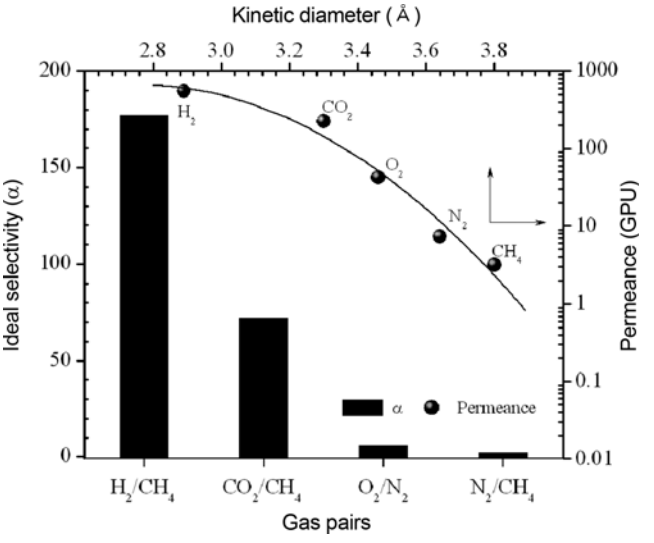

Figure 6. Permeance and ideal selectivities of various penetrant gases on commercial HF PI membrane.

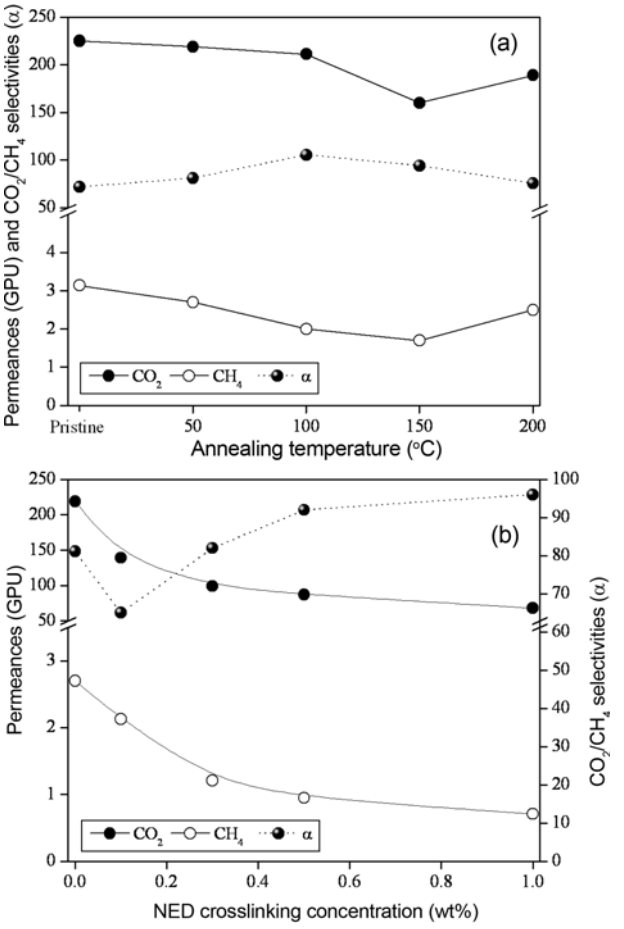

Figure 7. Permeation results of modified PI membranes (a) thermally annealed and (b) NED cross-linked.

feasibility of the selected commercial PI membrane for CO_2/CH_4 separation.

Gas Permeations in Thermally Annealed PI Membranes

Pure CO_2 and CH_4 permeation in thermally annealed PI membranes are shown in Figure 7(a). Permeances of both gases generally decreased as annealing temperature was increased to 150 °C then slightly increased at 200 °C. These results were slightly different from the general trends observed in previous studies were both gases showed continuous decrease in permeation at increasing annealing temperature [10,12,20]. However, this finding is consistent with the obtained FE-SEM, density and DMA results presented earlier. The slight permeance increase in PI annealed at 200 °C is due to the presence of macrovoids. This resulted to a modest selectivity improvement of 5 % compared to pristine PI. Highest selectivity was observed in PI annealed at 100 °C which is 46 % higher than the unmodified PI. The obtained selectivity (PI annealed at 100 °C α=106) was higher than the previously reported values [10,38,39]. These results suggest that annealing temperature for the commercial PI is best performed at 100 °C to attain the highest improvement in CO_2/CH_4 α while thermal annealing of PI near its T_g value was found unfavorable for the gas separation property of the membrane. Nonetheless, the obtained results demonstrate the potential of the annealed commercial PI membrane for CO_2/CH_4 separation.

Gas Permeations on Chemically Cross-linked PI Membranes

Cross-linking of PI membranes has often resulted to lower gas permeation due to the reduction of PI chain mobility as a consequence of the formation of interchain covalent bonds [21]. Because it is not easy to identify the dominating process on which NED is incorporated to the PI chain (as shown in Figure 1), the degree of cross-linking was not calculated in this study. Nonetheless, Figure 7(b) demonstrates the trade-off between gas permeances and NED concentration. This result suggests that increasing NED concentration resulted to higher degree of cross-linking which led to the reduction in gas permeances [34]. As mentioned earlier, high selectivity could increase the competence of the membrane to other separation methods but enhanced selectivity with low reduction in permeances is more desirable. Compared to the pristine PI membrane, CO_2 permeances were reduced by 38-70 % while CH_4 showed 32-77 % reduction. Permeance reductions led to enhanced selectivities from 72 of pristine PI to 82-96 of NED cross-linked PI. On the other hand, selectivity of PI treated with 0.1 wt% NED was remarkably lower than the pristine PI. At this point, it is not clear why this result was obtained but the abrupt decrease in CO_2 relative to CH_4 permeance resulted to a lower α=62. For improved selectivity with modest permeance reduction, the results suggest that 0.5 wt% NED is the optimal concentration for PI cross-linking. Compared to the thermally annealed membrane at 100 °C, permeance reductions in NED cross-linked PI were higher but the selectivity improvements were not as remarkable. From these results, NED can be used in PI cross-linking to improve PI α but thermal annealing presents a simpler yet more effective technique of attaining better membrane performance.

Thus, NED cross-linked PI membranes were subjected to post-treatment by thermal annealing at elevated temperatures to observe if it will improve the performance of the NED cross-linked PI membranes.

Gas Permeations in Thermally Induced NED Cross-linked PI Membranes

Permeation results from thermally induced NED cross-linked PIs are shown in Figure 8 using 0.5 wt% NED concentration. Thermal annealing of cross-linked PI resulted to further decrease in permeances. In Figure 3, FE-SEM images of thermally induced NED cross-linked PIs are shown. In Figure 3(g), the skin layer of NED treated PI annealed at 100 °C apparently disappeared. However, a dense phase is evident at the outer portion of the membrane.

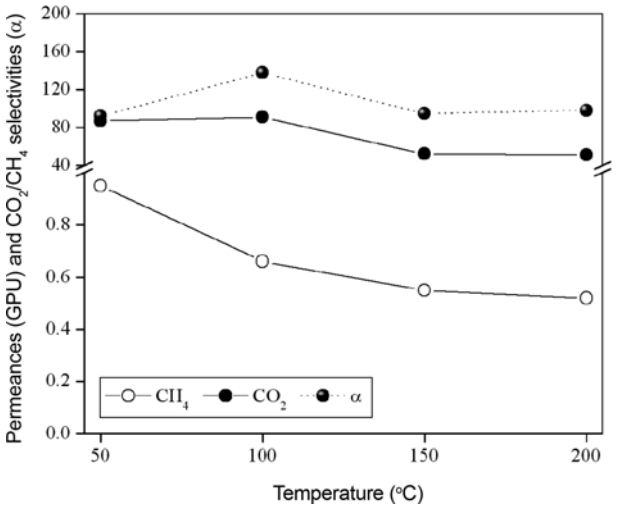

Figure 8. Permeation results of 0.5 wt% NED cross-linked PI annealed at different temperatures.

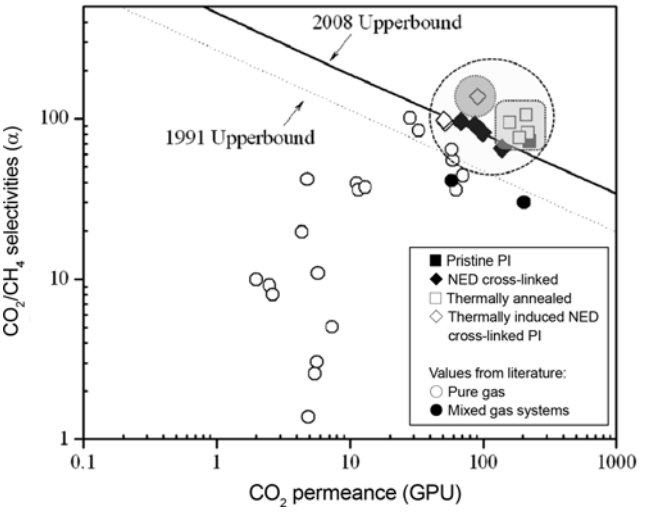

Figure 9. Robeson's plot showing the performances of all tested membranes in this study as compared to other reported values of CO_2 permeance and CO_2/CH_4 selectivities.

Thermal treatment enhanced the reactivity of NED, which facilitated the 'blending' of skin layer with the subsurface porous section. This becomes more evident at higher temperature (200 °C) as shown in Figure 3(h) where the dense phase appears to be thicker concomitant with the disappearance of pores at the outer portion of the membrane.

The enhanced cross-linking reaction between PI and NED at higher temperature resulted to remarkable decline in CH_4 permeance which improved CO_2/CH_4 selectivity. At 100 °C annealing temperature, CO_2 permeance was similar with that of cross-linked PI annealed at 50 °C while CH_4 permeance continuously decreased. This resulted to α value of 138, which is a 92 % improvement from the pristine PI, 30 % improvement from the thermally annealed PI at 100°C and 50 % improvement from the NED cross-linked PI post-treated at 50 °C. This is attributable to the simultaneous formation of CTCs and promotion of cross-linking reaction which allowed better interaction between NED and PI [3,20]. However, annealing at ≥150 °C resulted to more intense NED cross-linking which greatly affected the CO_2 permeance more than that of CH_4 and this led to the decline in selectivities from 138 to 95.

Overall Performances of the Investigated HF PI Membranes

In Figure 9, Robeson's plot shows the performances of all membranes tested in this study [40,41]. Compared to the membrane performances obtained in the literature [6,29,42], all of the tested membranes are located at the 2008 upper bound line including that of the unmodified commercial HF PI membrane. Thermally annealed PIs were within the same region as the pristine PI (enclosed box in Figure 9). On the other hand, NED cross-linked PI membranes had lower CO_2 permeances but improved selectivities. Lowest CO_2 permeances were obtained from thermally induced NED cross-linked membranes but highest α were also exhibited by these membranes. Among the tested samples, exceptional performances were attained by two membranes. These are thermally annealed PI at 100 °C (P/L=211, α=106) and PI cross-linked with 0.5 wt% NED which was thermally annealed at 100 °C (P/L=91, α=138). Highest α was obtained in 0.5 wt% NED cross-linked PI thermally annealed at 100 °C, but thermally annealed PI at 100 °C had higher CO_2 permeance. Thus, depending on the application, these two modified PI membranes are the best candidates for CO_2/CH_4 separations.

Conclusion

Modification of commercially available membrane was proven a convenient technique to tailor PI membrane properties for specific applications. Both thermal and chemical modifications remarkably improved the HF PI membrane performance in terms of CO_2 permeance and CO_2/CH_4 selectivity. However, since pure gas systems were tested in this study, further investigations using actual gas mixtures are necessary to determine the behavior of the modified membranes under realistic conditions and to observe CO_2 plasticization in more detail as it often causes a decline in membrane performance.

Acknowledgements

This work was supported by The Priority Research Centers Program [No. 2010-0028300] through The National Research Foundation of Korea (NRF) funded by the Korea Government, Ministry of Education Science and Technology (MEST) and the outcome of a Manpower Development Program for Energy & Resources supported by the Ministry of Knowledge and Economy (MKE) [2008-E-AP-HMP-170000].

References

1. J. D. Wind, D. R. Paul, and W. J. Koros, *J. Membr. Sci.*, **228**, 227 (2004).
2. S. Li, G. Alvarado, R. D. Noble, and J. L. Falconer, *J. Membr. Sci.*, **251**, 59 (2005).
3. J. D. Wind, C. Staudt-Bickel, D. R. Paul, and W. J. Koros, *Macromolecules*, **36**, 1882 (2003).
4. R. W. Baker, *Ind. Eng. Chem. Res.*, **41**, 1393 (2002).
5. Q. H. Zhang, W. Q. Luo, L. X. Gao, D. J. Chen, and M. X. Ding, *J. Appl. Polym. Sci.*, **92**, 1653 (2004).
6. J. Ren, R. Wang, T. S. Chung, D. F. Li, and Y. Liu, *J. Membr. Sci.*, **222**, 133 (2003).
7. J. N. Barsema, G. C. Kapantaidakis, N. F. A. van der Vegt, G. H. Koops, and M. Wessling, *J. Membr. Sci.*, **216**, 195 (2003).
8. C. Cao, T. S. Chung, Y. Liu, R. Wang, and K. P. Pramoda, *J. Membr. Sci.*, **216**, 257 (2003).
9. M. Al-Masri, D. Fritsch, and H. R. Kricheldorf, *Macromolecules*, **33**, 7127 (2000).
10. H. Kawakami, M. Mikawa, and S. Nagaoka, *J. Membr. Sci.*, **118**, 223 (1996).
11. Y. Xiao, L. Shao, T. S. Chung, and D. A. Schiraldi, *Ind. Eng. Chem. Res.*, **44**, 3059 (2005).
12. F. Zhou and W. Koros, *Polymer*, **47**, 280 (2006).
13. S. S. Hosseini and T. S. Chung, *J. Membr. Sci.*, **328**, 174 (2009).
14. S. Basu, A. Cano-Odena, and I. F. J. Vankelecom, *Sep. Purif. Technol.*, **75**, 15 (2010).
15. S. Matsui, H. Sato, and T. Nakagawa, *J. Membr. Sci.*, **141**, 31 (1998).
16. S. Saimani and A. Kumar, *J. Appl. Polym. Sci.*, **110**, 3606 (2008).
17. B. T. Low and T. S. Chung, *Carbon*, **49**, 2104 (2011).
18. A. M. W. Hillock and W. J. Koros, *Macromolecules*, **40**, 583 (2007).
19. L. Shao, L. Liu, S. X. Cheng, Y. D. Huang, and J. Ma, *J. Membr. Sci.*, **312**, 174 (2008).
20. L. Shao, T. S. Chung, S. H. Goh, and K. P. Pramoda, *J. Membr. Sci.*, **256**, 46 (2005).
21. M. E. Rezac, E. T. Sorensen, and H. W. Beckham, *J. Membr. Sci.*, **136**, 249 (1997).
22. C. H. Lau, B. T. Low, L. Shao, and T. S. Chung, *Int. J. Hydrogen Energ.*, **35**, 8970 (2010).
23. G. Dong, H. Li, and V. Chen, *J. Membr. Sci.*, **369**, 206 (2011).
24. Y. Xiao, T. S. Chung, and M. L. Chung, *Langmuir*, **20**, 8230 (2004).
25. Y. Liu, R. Wang, and T. S. Chung, *J. Membr. Sci.,* **189**, 231 (2001).
26. R. H. Perry and D. W. Green, "Perry's Chemical Engineering Handbook", 7th ed., McGraw-Hill Book Co., Singapore, 1997.
27. R. C. Reid, J. M. Prausnitz, and B. E. Poling, "The properties of Gases and Liquids", 4th ed., pp.11-149, McGraw-Hill Book Co., Singapore, 1987.
28. L. Meng and Y. Y. Duan, *Fluid Phase Equilibr.*, **238**, 229 (2005).
29. I. C. Omole, R. T. Adams, S. J. Miller, and W. J. Koros, *Ind. Eng. Chem. Res.*, **49**, 4887 (2010).
30. M. Peer, S. M. Kamali, M. Mahdeyarfar, and T. Mohammadi, *Chem. Eng. Technol.*, **30**, 1418 (2007).
31. M. D. Halls, C. P. Tripp, and H. B. Schlegel, *Phys. Chem. Chem. Phys.*, **3**, 2131 (2001).
32. S. H. Hsiao and K. H. Lin, *J. Polym. Sci. Polym. Chem.*, **43**, 331 (2005).
33. A. Iwasaki, A. Fujii, T. Watanabe, T. Ebata, and N. Mikami, *J. Phys. Chem.*, **100**, 16053 (1996).
34. Y. Liu, T. S. Chung, R. Wang, D. F. Li, and M. L. Chung, *Ind. Eng. Chem. Res.*, **42**, 1190 (2003).
35. J. P. La Femina, G. Arjivalingam, and G. Hougham, *J. Chem. Phys.*, **90**, 5154 (1989).
36. S. Tamai and A. Yamaguchi, *Polymer*, **37**, 3683 (1996).
37. S. H. Hsiao and Y. J. Chen, *Eur. Polym. J.*, **38**, 815 (2002).
38. K. Matsumoto, P. Xu, and T. Nishikimi, *J. Membr. Sci.*, **81**, 15 (1993).
39. E. R. Hensema, M. H. V. Mulder, and C. A. Smolders, *J. Appl. Polym. Sci.*, **48**, 2081 (1993).
40. L. M. Robeson, *J. Membr. Sci.*, **62**, 165 (1991).
41. L. M. Robeson, *J. Membr. Sci.*, **320**, 390 (2008).
42. S. S. Hosseini, N. Peng, and T. S. Chung, *J. Membr. Sci.*, **349**, 156 (2010).